Agostino Stilli, Helge A. Wurdemann and Kaspar Althoefer, A Novel Concept for Safe, Stiffness-Controllable Robot Links, Soft Robotics, Mary Ann Liebert, Inc. 2016 (accepted for publication 29 April 2016).

A Novel Concept for Safe, Stiffness-Controllable Robot Links

Agostino Stilli, Helge A. Wurdemann and Kaspar Althoefer*, *Member, IEEE*

***Abstract* — The recent decade has seen an astounding increase of interest and advancement in a new field of robotics, aimed at creating structures specifically for the safe interaction with humans. Softness, flexibility and variable stiffness in robotics have been recognised as highly desirable characteristics for many applications. A number of solutions were proposed ranging from entirely soft robots (such as those composed mainly from soft materials such as silicone), via flexible continuum and snake-like robots, to rigid-link robots enhanced by joints that exhibit an elastic behaviour either implemented in hardware or achieved purely by means of intelligent control. Although these are very good solutions paving the path to safe human-robot interaction, we propose here a new approach which focuses on creating stiffness controllability for the linkages between the robot joints.**

This paper proposes a replacement for the traditionally rigid robot link – the new link is equipped with an additional capability of stiffness controllability. With this added feature, a robot can accurately carry out manipulation tasks (high stiffness), but can virtually instantaneously reduce its stiffness when a human is nearby or in contact with the robot. The key point of the invention described here is a robot link made of an airtight chamber formed by a soft and flexible, but high-strain resistant combination of a plastic mesh and silicone wall. Inflated with air to a high pressure, the mesh-silicone chamber behaves like a rigid link; reducing the air pressure, softens the link and rendering the robot structure safe.

This paper investigates a number of link prototypes and shows the feasibility of the new concept.

Stiffness tests have been performed, showing that a significant level of stiffness can be achieved - up to 40 N reaction force along the axial direction, for a 25 mm diameter sample at 60 kPa, at an axial deformation of 5 mm. The results confirm that this novel concept to linkages for robot manipulators exhibits the beam-like behaviour of traditional rigid links when fully pressurised and significantly reduced stiffness at low pressure. The proposed concept has the potential to easily create safe robots, augmenting traditional robot designs.

I. Introduction

In the past decades, the introduction of soft robotics has redefined the limits of what a robot can accomplish. A number of soft, rubber or silicone-based manipulators have proved capable of achieving complex body poses [1], performing whole-body manipulation [2] and exhibiting articulated movements using simple mechanical structures [3], [4].

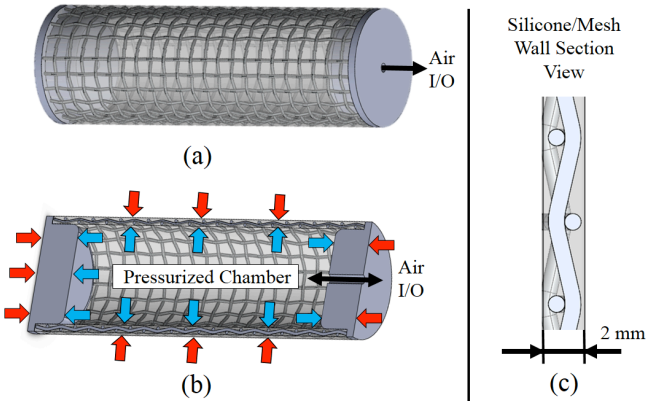

Figure 1: CAD drawings of the stiffness-controllable link: overview of the link assembly (a), longitudinal section view of the link (b) showing the I/O channel for pressurized air, with azure arrows showing the force distribution of the pressurized air inside the internal chamber and red arrows the force distribution of the reaction forces of the link. (c) subfigure shows a longitudinal magnified section of the wall link, showing the mesh embedded in a 2 mm silicone layer.

Many silicone-based robotic systems make use of pneumatic actuation: a number of chambers independently actuated [5] or connected in a network [6] are directly embedded in the silicone body of the robot. The controlled expansion or contraction of the pressurised chambers leads to a deformation and, thus, movement of the overall structure [7]. The main limitation of this type of actuation is the maximum acceptable deformation of the robot body and the maximum fluidic (pneumatic or hydraulic) pressure that its silicone structure is able to withstand without bulging or even blowing up.

As a consequence of these mechanical limitations the maximum force exertable by such robotic systems is typically limited [1]. A deformation of the same relative order of magnitude is produced in the legs of the walking soft robot proposed in [7] once its pneumatic network is pressurised to perform a movement. These volume variations are generally difficult to model and thus difficult to predict, creating a significant control problem.

The STIFF-FLOP project (EU FP7 - Grant n. 287728) attempted to overcome this issue developing bio-inspired soft robotic surgical tools [8], [9]. The proposed modular manipulator in STIFF-FLOP was made out of silicone. Each module comprised of three equally spaced pneumatically actuated chambers in parallel to the longitudinal axis [10]. The STIFF-FLOP manipulator has embedded sensors such as F/T sensors and bending sensors to estimate the robot's tip pose [11]–[14]. To limit the lateral inflation of the

*A. Stilli and are with the Department of Informatics, King's College London, Strand, London WC2R 2LS, UK (e-mail: agostino.stilli@kcl.ac.uk)

K. Althoefer is with the School of Engineering and Materials Science, Queen Mary University of London, Mile End Rd, London E1 4NS, UK (e-mail: k.althoefer@qmul.ac.uk)

H. Wurdemann is with the Department of Mechanical Engineering, University College London, Torrington Place, London WC1E 7JE (email: h.wurdemann@ucl.ac.uk)

modules, each chamber was individually fibre-reinforced [15], significantly improving the performance compared to externally braided robots [5]. A similar approach has been investigated in [16], where the combination of different braiding angles was explored to achieve a desired bending behaviour for the robot. The usage of external meshes for soft robotic fingers has been explored by researchers in [17], [18].

To overcome the issue of large deformations associated with the pneumatic actuation of silicone based robot manipulators the authors of this paper have introduced in [19], [20] a new type of soft robot, called the Inflatable Arm, composed of an inner silicone bladder with an outer non-extendable sleeve. The purpose of the sleeve is to further minimise undesired deformations of the soft body of the robot, constraining a deformable system into a non-extendable enclosure. Tendons attached to the outer sleeve at various locations allow the inflatable arm to be steered. It is noted that the robot employs a hybrid antagonistic actuation combining the advantages of pneumatic and tendon-driven systems. Most importantly, the bio-inspired arm is able to change its stiffness by concurrently regulating the chamber pressure and the extension of the tendons.

Here, we propose and investigate a new type of silicone-based stiffness-controllable, inflatable robotic link, using pneumatics. The work presented here follows the overall idea of creating inherently safe robots that can be used in modern industrial or surgical settings, attempting to provide solutions for safe human robot interaction. In our envisaged solution, these inflatable links are the connecting elements between robot manipulator joints (possibly actuated by traditional electric motors, series elastic actuators or even fluidic actuators), replacing common, rigid robotic links. This paper describes the fabrication process and stiffness analysis of these novel links. Figure 1 shows the design and the working principle of the proposed link: a mesh is embedded in the lateral wall of a silicone cylinder, preventing it from expanding laterally and longitudinally once pressurised air is injected in the central chamber. We investigate the dependence between the design parameters of the mesh and the stiffness of the link.

This paper is organized as follows: The design of the stiffness-controllable link and its fabrication process is presented in Section II. The investigation focussed on the silicone materials and meshes to be used, to achieve adequate behaviour for the main states of these links – soft and stiff.. In Section III the experimental setup for stiffness evaluation is described and results presented. Section IV summarises the conclusions and achievements of this paper and proposes future work and potential applications for the new concept.

II. Materials and Methods

The novel link is composed of two main structural elements: a plastic mesh embedded inside a layer of silicone in the shape of a hollow cylinder. When both ends of this cylindrical structure are closed, airtight chambers that can be pressurised are being achieved. Although its inflation is limited both in the longitudinal and radial direction by the inextensible mesh as shown in the force scheme of Figure 2, the mesh gives shape to the cylindrical link and prevents it from collapsing when it is in a low pressure state. Exploring the influence on the stiffness of this type of link, a number of different silicone materials and plastic meshes were investigated at different pressure levels.

The proposed novel link is designed to be:

- stiffness controllable and inherently safe
- easy to manufacture and inexpensive
- made of soft material, but capable of behaving similar to a traditional rigid link
- hollow, so to maximise the housing space inside the link body
- lightweight, being made of a plastic mesh, silicone and pressurised with air.

A. Analysis of Mesh and Silicone Properties

To select a mesh suitable for this application, a number of parameters such as the shape and the aperture size of the patterns, as well as the material and diameter of the mesh threads were considered.

Polypropylene (PP) mesh material is chosen as it is durable and does not react chemically with silicone based materials. In addition, the surface of these meshes is smooth, hence, the risk of perforation of the silicone membrane is considerably reduced. The low cost of these meshes allows the creation of inexpensive but robust and lightweight robotic links. Furthermore any link diameter can be easily realised using the proposed fabrication process. A diamond shaped aperture pattern was chosen for our application. This mesh aperture geometry was chosen among other commercially available meshes with different patterns due to its isotropic mechanical behaviour and its negligibly low elasticity. These features match our requirements in terms of non-deformability of the link along longitudinal and radial directions.

Based on these considerations, four different diamond meshes from Normesh Ltd.[1] with different aperture sizes and thread diameters have been selected.

With regards to the selection of an appropriate silicone material, different silicone types (Dragon Skin®, Oomoo® and Ecoflex®) were evaluated concerning their stiffness, chemical stability and castability. Based on our analysis, we selected Dragon Skin® which proved to be most suitable exhibiting a good level of elasticity and shape retention. Aiming to achieve a good trade-off between softness of the material and mechanical rigidity of the cylindrical structure, Dragon Skin® 20A was selected.

B. Fabrication Procedure Stiffness-Controllable Link Samples

Concerning the meshes, we evaluated four PP meshes with aperture sizes between 105μm and 420μm, and corresponding thread diameters between 106μm and 340μm.

[1] Normesh Ltd.: http://www.normesh.co.uk/da/111262, accessed on 30 June 2015.

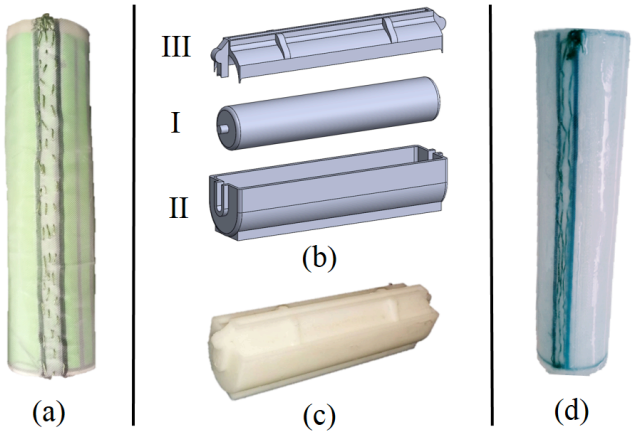

Figure 2: Fabrication stages of the link: mesh sewn in the shape of a cylinder (a), mould components (I, II and III (b)) and mould assembled (c). Figure (d) shows the link after demoulding and removing of the silicone excess.

Rectangular sheets of the selected PP meshes of dimensions of 15cm × 8.5cm were sewn in the shape of cylinders with a length of 15cm and a diameter of 2.5cm to create the link prototypes. Nylon threads were used to sew the longitudinal mesh sides together (with an overlap of 7 mm) to form the cylindrical structures (see Figure 2 (a)). The meshes were cut and sewn in a way that the main diagonal of the diamond apertures are aligned with the longitudinal axis of the link. A mould consisting of three components was created to allow each cylindrical mesh to be enclosed within the silicone-based material. The mould parts I, II and III (see Figure 2 (b)) were created by a Stratasys Dimension SST 768 rapid prototyping machine. The moulding process is as follows: the sewn PP mesh is slipped over the cylindrical mould component I. Then, a silicone mixture is prepared and degassed in a vacuum chamber. Part of the silicone mixture is then poured into the base part of the mould (II), filling it for half of its capacity. Part I of the mould with the mesh is then inserted from the top into part II. More silicone is added after inserting part I into part II, to make sure that enough material is present to form a complete and continuous link wall. Part III is then inserted into part II as shown in Figure 2(b); excess silicone escapes from the long aperture located at the top of part III. The silicone is then allowed to cure at room temperature for 8 hours. Figure 2(c) shows the mould in its assembled state. Figure 2(d) shows the link after the moulds and any excess silicone has been removed. The whole procedure was repeated to create four samples employing the four different meshes.

Table 1 summarises the characteristics of the samples including the mesh aperture size, wall thickness and thread diameter. The mould was designed on purpose in a way to generate silicone-mesh walls of the same thickness for all four samples, regardless of the thickness of the used mesh.

III. Experimental Setup and Results

A test rig was prepared to evaluate the stiffness of the prototypes according to different levels of pressure applied. This investigation was aimed at understanding which mesh property impacted mostly on the overall stiffness of the system: the aperture size or the diameter of the thread used.

Table 1: Variable stiffness link samples, with corresponding mesh aperture sizes and thread diameter embedded in Dragon Skin® 20A silicone.

Sample	Aperture Size	Thread Diameter	Wall Thickness
(a)	105µm	106µm	2 mm
(b)	150µm	110µm	2 mm
(c)	250µm	215µm	2 mm
(d)	420µm	340µm	2 mm

In order to pressurise and test the samples, one of the two circular openings in the base of the cylinder was sealed using a customized 3D printed cap. The cap was inserted and secured in place with cable ties and silicone glue to guarantee the internal chamber to be air-tight. Figure 3 (a) shows one of the samples ready for testing. After closing the tip with the cap, the open end of the sample was attached to a customised 3D printed test base. A pressure line is embedded in the base and connected to a pressure regulator (SMC ITV0010-3BS-Q). This allows the control of the pressure level inside the link. Figure **3**3 displays the experimental setup of the system for a lateral tip stiffness test. Cable ties and silicone glue were used on the base side as well to ensure that the only air inlet/outlet is via the pressure line. The pressure regulator was controlled by LabVIEW software. The level of stiffness of the samples was evaluated at the tip, where the displacement generated by an external applied force is maximal. Tests were performed pushing an ATI Nano17 Force/Torque sensor connected to a linear module towards the tip as shown in Figure 3 - laterally along the *x*-axis and longitudinally at the front of the tip along the *z*-axis. To measure F_z, a linear slide was rotated counter-clockwise by 90° in comparison with the pose shown in Fig. 3, so that the linear module with the mounted F/T sensor exerts forces along the *z*-axis direction.

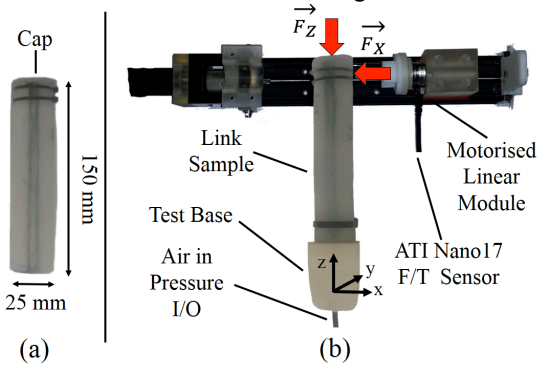

Figure 3: Link sample with 3D printed cap embedded for stiffness test (a) and setup for the lateral stiffness tests at the tip (b): direction of the lateral force Fx and of the longitudinal force Fz applied during the tests are marked.

Both test scenarios have been performed applying four different pressure levels of 15 kPa, 30 kPa, 45 kPa and 60 kPa. Each experiment started with the ATI Nano17 F/T sensor being 0.5 mm away from the silicone surface of the

sample. The lateral stiffness tests consisted of load and unload cycles achieving a deflection of 15 mm. For longitudinal stiffness tests a smaller displacement of 5 mm was achieved so to avoid buckling phenomena. Each loading/unloading cycle was performed five times to compute the variance of the measurements. It is important to note that no significant radius or length variations occurred after pressurising the samples, further proving the effectiveness of this design in terms of limitation of undesirable deformations of this silicone based system.

A. Stiffness Evaluation - Lateral Tip Test

For each of the four link samples, the lateral tip test has been performed applying four different pressure levels. Each loading and unloading cycle was repeated five times. The results of these tests are shown in Figure 4 with the deflection displacement plotted against force.

In Figure 3, the average values of the five force reading cycles are plotted with the corresponding error bars for each pressure level in separate graphs. As shown in Figure 4 (a), the load-unload curves have an overall linear trend and some hysteresis. The maximum achievable force is 2.09 N at 15 kPa. Increasing the pressure to 30 kPa, 45 kPa and 60 kPa, the force increases to 2.61 N, 2.85 N and 3.01 N, respectively. As expected, applying a larger pressure, leads to an increase in stiffness of the inflated link and, thus, an increase of lateral reaction force. Comparing the graphs of Figures 5, showing the readings obtained from experiments with a different mesh-silicone combination, it can be deduced that the bigger the thread diameter and the aperture sizes are, the stiffer is the inflated link. For instance, the mesh used in Figure 5 (a) at 60 kPa exerts a lateral force of 3.01 N whereas the one used in Figure 5 (d) with the same level of internal pressure can exert more than double the amount of reaction force at 6.55 N, with the same displacement.

B. Stiffness Evaluation – Longitudinal Tip Tests

The results of the stiffness tests for the four links along the longitudinal direction on the tip are shown in Figures 5(a)-(d). Each graph shows force values against tip displacement, calculated as the average of five load-unload cycles for four different pressure levels. Error bars are included.

Comparing Figures 4 and 5, it is clear that the forces measured at a displacement of 5 mm for the longitudinal tip stiffness tests exceeded consistently the corresponding measurements of the lateral stiffness tests. For instance the link shown in Figure 5 (a) pressurised at 15 kPa produces a maximum reaction force of 2.09N, if stressed laterally, with a displacement of 15 mm; however, the same link sample leads to a peak reaction force of 11.90 N and an associated displacement of 4.2mm only, when the force is applied longitudinally (see Figure 6(a)). Thus, the sample behaves in a similar manner to a rigid beam, particularly one with a circular section. The mechanical properties of this soft robotic link structure make the modelling significantly simpler when compared to the typical silicone based robot manipulators. It is important to note that the peak force values during a load-unload cycle are reached for the longitudinal tests before the displacement of 5 mm is reached. Once again this can be explained considering the system as a cantilever beam(clamped on one base, free at the other end). The compression force along the longitudinal axis produces buckling behaviour after a deformation of 3.5-4.5 mm; the beginning of the buckling corresponds to the trend inversion in the exerted force. Also in this case, the obtained force readings for the four prototypes display a continuous increase considering the increasing pressure levels as shown in Figure **5**5. Furthermore, the link prototypes composed of meshes with bigger threads and aperture sizes exhibit a stiffer behaviour. Table 2 summarises the experimental results.

IV. CONCLUSIONS

Departing from the traditional approach to robot arms with their rigid links, this paper proposes a novel concept for stiffness-controllable robot links. The proposed concept is inspired by our earlier work on inflatable, stiffness-controllable robotic manipulators [19].

The proposed concept provides a new solution to vary the stiffness of robot manipulator links with ramifications especially in the area of safe human-robot interaction (HRI). In contrast to current solutions for safe HRI employing stiffness-controllable joints such as those based on variable elastic actuators, we pursue a different approach here where the links are the focus of our attention and whose stiffness can be controlled to adapt to the environmental situations, especially to render the robot safe when, for example, a human is in the nearby vicinity, by rapidly reducing the stiffness.

As presented in this paper, we propose our stiffness-controllable link concept as a replacement of the rigid links of traditional robot arms. We believe that our approach is advantageous because we consider turning a standard joint into one with compliant features a more complicated approach. One can, though, conceive a robot arm design which combines our stiffness-controllable links with joints whose compliance is also controllable, if required. Additional advantages of the proposed concept are:

- High rigidity with low deformation when pressurised,
- Light-weight, low-inertia structure,
- Ample of space inside the inflatable-link that can be used for cabling,
- Opportunity to estimate interaction forces based on measured pressure within the inflatable links.

The last point is particularly useful in the context of safety, since a controller with pressure feedback can be easily implemented to depressurise the manipulator links when an impact is detected, to cushion a collision with a human appropriately, considerably reducing the risk of injury. Hence, the proposed link concept is especially suitable for applications that involve human-robot interaction and collaboration

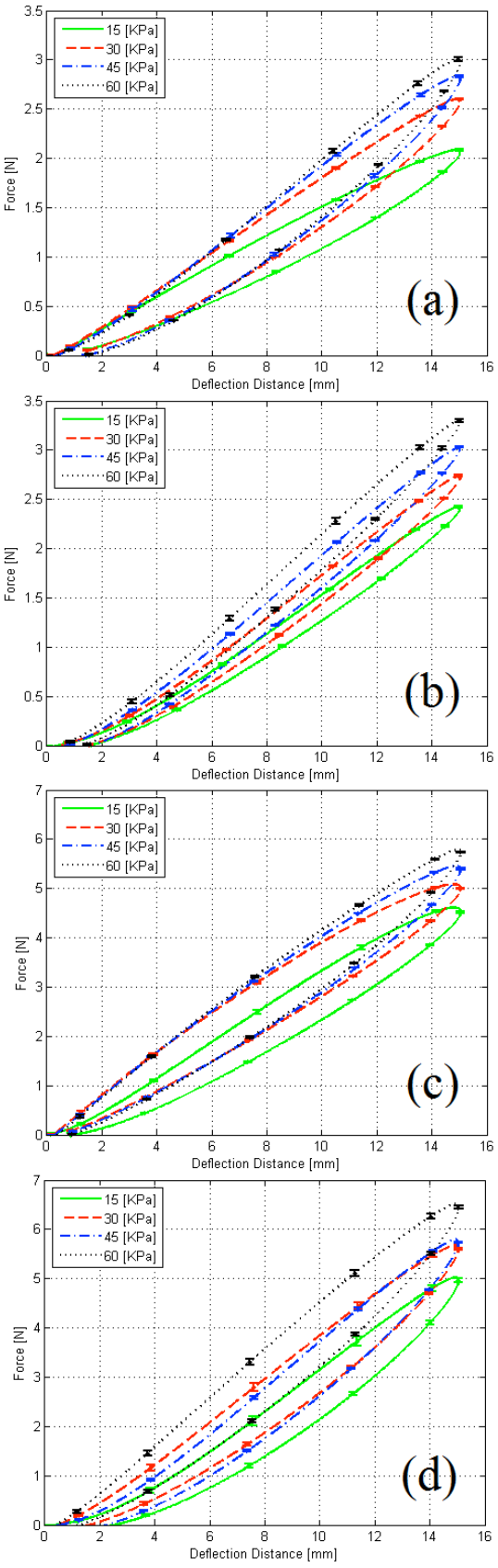

Figure 4: Deflection distance versus force at the link tip laterally applied for samples (a), (b), (c) and (d) at 15 KPa, 30 KPa, 45 KPa and 60 KPa. Standard deviation values ordered by increasing pressure level: (a) 0.007, 0.006, 0.0144, 0.009; (b) 0.009, 0.008, 0.008, 0.018; (c) 0.018, 0.016, 0.013, 0.016; (d) 0.041, 0.039, 0.017, 0.036.

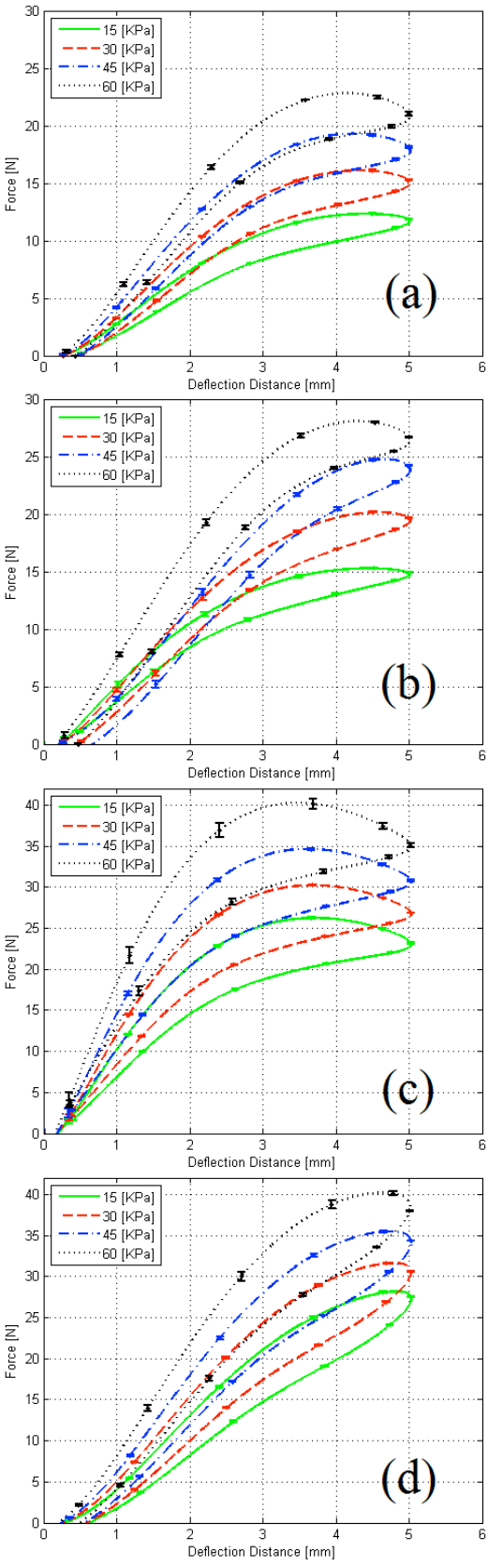

Figure 5: Deflection versus force at the link tip longitudinally applied for samples (a), (b), (c) and (d) at 15KPa, 30KPa, 45KPa and 60KPa. Standard deviation values ordered by increasing pressure level: (a) 0.051, 0.080, 0.089, 0.153; (b) 0.150, 0.136, 0.178, 0.179; (c) 0.133, 0.123, 0.206, 0.536; (d) 0.095, 0.100, 0.121, 0.255.

Table 2: Comparison of peak force values at different pressure levels for the four samples analysed in the lateral and longitudinal stiffness test. Colour gradients show force trends in relation to pressure levels and meshes geometrical characteristics.

Stiffness Test		Sample	Peak Forces [N]			
			15 kPa	30 kPa	45 kPa	60 kPa
Lateral Tip	Thread Diameter / Aperture Size	(a)	2.09	2.61	2.85	3.01
		(b)	2.42	2.73	3.03	3.30
		(c)	4.55	5.00	5.40	5.83
		(d)	5.04	5.71	5.81	6.55
Longitudinal Tip	Thread Diameter / Aperture Size	(a)	11.90	15.10	17.90	20.90
		(b)	14.90	19.50	23.70	26.50
		(c)	23.50	27.20	31.50	35.80
		(d)	27.80	31.10	34.70	39.10

V. Acknowledgments

This research has received funding from the European Commission's Seventh Framework Programme, project STIFF-FLOP under grant agreement No 287728 and from Horizon 2020 Research and Innovation Programme, project FourByThree under grant agreement No 637095. The authors would also like to acknowledge the King's College London, Centre for Robotic Research for the support of the experimental studies.

VI. Author Disclosure Statement

The authors here state that no competing financial interests exist.

References

[1] C. Laschi, M. Cianchetti, B. Mazzolai, L. Margheri, M. Follador, and P. Dario, "Soft Robot Arm Inspired by the Octopus," *Adv. Robot.*, vol. 26, no. 7, pp. 709–727, Jan. 2012.

[2] R. V Martinez, J. L. Branch, C. R. Fish, L. Jin, R. F. Shepherd, R. M. D. Nunes, Z. Suo, and G. M. Whitesides, "Robotic tentacles with three-dimensional mobility based on flexible elastomers.," *Adv. Mater.*, vol. 25, no. 2, pp. 205–12, Jan. 2013.

[3] H.-T. Lin, G. G. Leisk, and B. Trimmer, "GoQBot: a caterpillar-inspired soft-bodied rolling robot," *Bioinspir. Biomim.*, vol. 6, no. 2, p. 26007, 2011.

[4] K. Suzumori, S. Endo, T. Kanda, N. Kato, and H. Suzuki, "A bending pneumatic rubber actuator realizing soft-bodied manta swimming robot," in *Proceedings - IEEE International Conference on Robotics and Automation*, 2007, no. April, pp. 4975–4980.

[5] M. Cianchetti, T. Ranzani, G. Gerboni, I. De Falco, C. Laschi, and A. Menciassi, "STIFF-FLOP surgical manipulator: Mechanical design and experimental characterization of the single module," *IEEE Int. Conf. Intell. Robot. Syst.*, pp. 3576–3581, 2013.

[6] B. Mosadegh, P. Polygerinos, C. Keplinger, S. Wennstedt, R. F. Shepherd, U. Gupta, J. Shim, K. Bertoldi, C. J. Walsh, and G. M. Whitesides, "Pneumatic networks for soft robotics that actuate rapidly," *Adv. Funct. Mater.*, vol. 24, no. 15, pp. 2163–2170, 2014.

[7] R. F. Shepherd, F. Ilievski, W. Choi, S. A. Morin, A. A. Stokes, A. D. Mazzeo, X. Chen, M. Wang, and G. M. Whitesides, "Multigait soft robot," pp. 1–4, 2011.

[8] Y. Noh, S. Sareh, J. Back, H. A. Wü, T. Ranzani, E. Lindo, A. Faragasso, H. Liu, I. Member, and K. Althoefer, "A Three-Axial Body Force Sensor for Flexible Manipulators," 2014.

[9] S. Sareh, a Jiang, a Faragasso, Y. Noh, T. Nanayakkara, P. Dasgupta, L. D. Seneviratne, H. a Wurdemann, and K. Althoefer, "Bio-Inspired Tactile Sensor Sleeve for Surgical Soft Manipulators," pp. 1454–1459, 2014.

[10] T. Ranzani, M. Cianchetti, G. Gerboni, I. De Falco, G. Petroni, and A. Menciassi, "A modular soft manipulator with variable stiffness," no. September, pp. 11–14, 2013.

[11] H. A. Wurdemann, S. Sareh, A. Shafti, Y. Noh, A. Faragasso, D. S. Chathuranga, H. Liu, S. Hirai, and K. Althoefer, "Embedded electro-conductive yarn for shape sensing of soft robotic manipulators," in *Engineering in Medicine and Biology Society (EMBC), 2015 37th Annual International Conference of the IEEE*, 2015, pp. 8026–8029.

[12] Y. Noh, E. L. indo Secco, S. Sareh, H. Wurdemann, A. Faragasso, J. Back, H. Liu, E. Sklar, and K. Althoefer, "A continuum body force sensor designed for flexible surgical robotics devices," *Conf. Proc. ... Annu. Int. Conf. IEEE Eng. Med. Biol. Soc. IEEE Eng. Med. Biol. Soc. Annu. Conf.*, vol. 2014, pp. 3711–3714, 2014.

[13] S. Sareh, A. Jiang, A. Faragasso, Y. Noh, T. Nanayakkara, P. Dasgupta, L. D. Seneviratne, H. A. Wurdemann, and K. Althoefer, "Bio-inspired tactile sensor sleeve for surgical soft manipulators," in *Robotics and Automation (ICRA), 2014 IEEE International Conference on*, 2014, pp. 1454–1459.

[14] Y. Noh, S. Sareh, H. Wurdemann, H. Liu, J. Back, J. Housden, K. Rhode, and K. Althoefer, "Three-Axis Fiber-optic Body Force Sensor for Flexible Manipulators," *IEEE Sens. J.*, vol. 16(6), pp. 1641–1651, 2016.

[15] J. Fras, J. Czarnowski, M. Macias, J. Glowka, M. Cianchetti, and A. Menciassi, "New STIFF-FLOP module construction idea for improved actuation and sensing," *Robotics and Automation (ICRA), 2015 IEEE International Conference on*. pp. 2901–2906, 2015.

[16] A. A. M. Faudzi, M. R. M. Razif, I. N. A. M. Nordin, K. Suzumori, S. Wakimoto, and D. Hirooka, "Development of bending soft actuator with different braided angles," in *IEEE/ASME International Conference on Advanced Intelligent Mechatronics, AIM*, 2012, pp. 1093–1098.

[17] R. Deimel and O. Brock, "A Novel Type of Compliant , Underactuated Robotic Hand for Dexterous Grasping," *Proc. Robot. Sci. Syst.*, p. p18, 2014.

[18] V. Wall, R. Deimel, and O. Brock, "Selective stiffening of soft actuators based on jamming," *Robotics and Automation (ICRA), 2015 IEEE International Conference on*. pp. 252–257, 2015.

[19] A. Stilli, H. A. Wurdemann, and K. Althoefer, "Shrinkable, stiffness-controllable soft manipulator based on a bio-inspired antagonistic actuation principle," *Intelligent Robots and Systems (IROS 2014), 2014 IEEE/RSJ International Conference on*. pp. 2476–2481, 2014.

[20] F. Maghooa, A. Stilli, Y. Noh, K. Althoefer, and H. A. Wurdemann, "Tendon and pressure actuation for a bio-inspired manipulator based on an antagonistic principle," *Robotics and Automation (ICRA), 2015 IEEE International Conference on*. pp. 2556–2561, 2015.